

# Excitations of the bimodal Ising spin glass on the brickwork lattice

W. Atisattapong and J. Poulter

*Department of Mathematics, Faculty of Science, Mahidol University, Rama 6 Road, Bangkok 10400, Thailand*

(Dated: November 21, 2018)

An exact algorithm is used to investigate the distributions of the degeneracies of low-energy excited states for the bimodal Ising spin glass on the brickwork lattice. Since the distributions are extreme and do not self-average, we base our conclusions on the most likely values of the degeneracies. Our main result is that the degeneracy of the first excited state per ground state and per spin is finite in the thermodynamic limit. This is very different from the same model on a square lattice where a divergence proportional to the linear lattice size is expected. The energy gap for the brickwork lattice is obviously  $2J$  on finite systems and predicted to be the same in the thermodynamic limit. Our results suggest that a  $2J$  gap is universal for planar bimodal Ising spin glasses. The distribution of the second contribution to the internal energy has a mode close to zero and we predict that the low-temperature specific heat is dominated by the leading term proportional to  $T^{-2} \exp(-2J/kT)$ .

PACS numbers: 75.10.Hk, 75.10.Nr, 75.40.Mg, 75.60.Ch

## I. INTRODUCTION

Although bimodal planar Ising spin glass models are very simple in concept, they are extremely controversial. One main reason why concerns the energy gap between the ground and first excited states. To date, most work has been reported for the square lattice where there is wide acceptance for the scenario of a critical point only at zero temperature<sup>1,2</sup>. In the absence of any contradictory evidence or suggestion, we assume this to be the case for other planar models, including the brickwork lattice.

Bimodal models have bond (nearest-neighbor) interactions of fixed magnitude  $J$  and random sign. Both the ground and excited states have a very large degeneracy. For an infinite square lattice, without open boundaries, it is clear that any finite number of spin flips must either result in another ground state or an excited state with an increase in energy not less than  $4J$ . For the brickwork lattice the corresponding energy gap is clearly  $2J$ , since the lattice coordination number is three.

About 20 years ago, Wang and Swendsen<sup>3</sup> published evidence that the energy gap for the square lattice in the thermodynamic limit was  $2J$ . This flew in the face of the naive expectation of  $4J$ . Essentially, the claim was that it is possible for an infinite number of spin flips to provide an excited state with energy only  $2J$  above a ground state. The issue here is the noncommutativity of the zero-temperature and thermodynamic limits. The thermodynamic limit has to be taken first. Nevertheless, for the brickwork lattice we do not expect this to be an issue and the main interest of this paper is to show evidence that this is the case. Both models have the same energy gap in the thermodynamic limit, although the reasons why are quite different.

For the square lattice there are three scenarios in the literature regarding the energy gap. First, support for the  $2J$  energy gap includes work at finite temperatures involving exact computations of partition functions<sup>4</sup>, a worm algorithm<sup>5</sup> and Monte Carlo simulation<sup>6</sup>. Distributions of excited-state degeneracies

at arbitrary temperature<sup>7</sup> also indicate a  $2J$  gap. Essentially, it was shown that the degeneracy of the first excited state per ground state and per spin diverges in the thermodynamic limit. In consequence the  $4J$  gap of the finite system is reduced to  $2J$ .

Second, Saul and Kardar<sup>8</sup> reported that the energy gap should be  $4J$  as suggested by simple analysis. The third published scenario<sup>9</sup> basically claims that the energy gap approaches zero in the thermodynamic limit leading to power law behaviour for the specific heat. This possibility has been discussed at some length in Ref. 10, although clear conclusions remain unavailable due to difficulties related to finite lattice size and extrapolation to very low temperature.

The brickwork lattice (Fig. 1(a)) studied in this paper is logically equivalent to the hexagonal, or honeycomb, lattice (Fig. 1(b)). Very little work has been published to date, especially concerning the ground state. The ground state energy per bond has been quoted<sup>11</sup> as  $-0.82J$ . The entropy per spin has been reported by Aromsawa<sup>12</sup> as  $0.02827(5)k$  with an energy  $-1.2403(2)J$  per spin, in good agreement with Ref. 11. The spin glass phase is thought to exist for a concentration of negative bonds<sup>13</sup> above about 0.067. Work at finite temperature<sup>14,15,16</sup> places the multicritical, or Nishimori, point at the same concentration; in agreement if reentrant phase boundaries are absent.

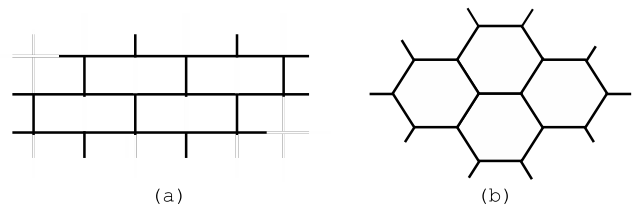


FIG. 1: (a) The brickwork lattice. (b) The equivalent hexagonal lattice.

Our calculations of the degeneracies of excited states for the brickwork lattice are exact. The temperature

is fixed and arbitrarily low; we do not use any numerical value. The lattice is constructed by taking a square lattice and diluting bonds in a regular manner to leave plaquettes with six perimeter bonds; logically equivalent to hexagons as shown in Fig. 1. The disorder realizations are independently quenched random configurations of negative bonds in a patch that contains all the frustrated plaquettes. Periodic boundary conditions are used in one dimension. The number of sites  $L$  for this dimension is necessarily even. The cylindrically wound frustrated patch is embedded in an infinite unfrustrated environment in the second dimension.

## II. FORMALISM

An algorithm based on the Pfaffian method<sup>17</sup> and degenerate state perturbation theory<sup>18,19,20</sup> for the square lattice was adapted to evaluate the degeneracies of excited states for the brickwork lattice. The main points of this procedure are given in the following. From the square lattice, we dilute bonds in a regular manner to define the brickwork lattice. Using the fermion decoration of bonds (one either side), a brickwork plaquette has eight fermions inside (filled circles) and six others across the bonds as shown in Fig. 2.

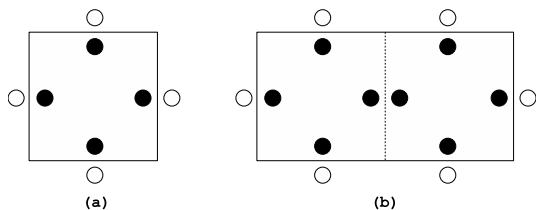


FIG. 2: (a) A square plaquette as in Ref. 20. (b) A brickwork plaquette obtained by dilution of the central bond (denoted by a dotted line) between two square plaquettes.

As for the bimodal Ising spin glass on the square lattice, the partition function is given by  $Z \sim (\det D)^{1/2}$  where  $D$  is a real skew-symmetric  $4N \times 4N$  matrix for a lattice with  $N$  sites.  $D$  is a singular matrix at zero temperature with zero eigenvalues which are equal in number to the number of frustrated plaquettes. Each eigenvalue approaches zero according to the form

$$\epsilon = \pm \frac{1}{3} X \exp(-2Jr/kT), \quad (1)$$

where  $r$  is an integer (an order of perturbation theory) and  $X$  is a real number. The quantities  $r$  and  $X$  can be exactly evaluated by degenerate state perturbation theory. The ground-state energy and entropy of the system can be defined similarly as for the square lattice<sup>19</sup>. It is equivalent to expressing the ground-state degeneracy as

$$M_0 = \prod X. \quad (2)$$

where the product is over all the positive defect eigenvalues.

The gauge-invariant method is applied similarly as for the square lattice<sup>19</sup> to separate the singularities of  $D$  for the brickwork lattice using real matrices as follows. At zero temperature, the perfect system (no frustration) Green's function<sup>19</sup>  $g_0$  is obtained by transforming  $D$  into a plane-wave basis and inverting an  $8 \times 8$  matrix. The nonzero elements of  $g_0$  are only across bonds and localized inside plaquettes. Across bonds we have  $g_0(+, -) = -g_0(-, +) = \frac{1}{2}$  where the matrix indices are defined in Fig. 4 of Ref. 19. Within a plaquette  $g_0$  is as given by the following matrix<sup>12</sup>:

$$g_0 = \frac{1}{2} \begin{bmatrix} 0 & -1 & 1 & -1 & 1 & 1 & -2 & 0 \\ 1 & 0 & 1 & -1 & 1 & 1 & 0 & 2 \\ -1 & -1 & 0 & -1 & 1 & 1 & -2 & 0 \\ 1 & 1 & 1 & 0 & 1 & 1 & 0 & 2 \\ -1 & -1 & -1 & -1 & 0 & 1 & -2 & 0 \\ -1 & -1 & -1 & -1 & -1 & 0 & 0 & -2 \\ 2 & 0 & 2 & 0 & 2 & 0 & 0 & 2 \\ 0 & -2 & 0 & -2 & 0 & 2 & -2 & 0 \end{bmatrix} \quad (3)$$

where the elements of  $g_0$  are with respect to the bond basis of a plaquette as shown in Fig. 3.

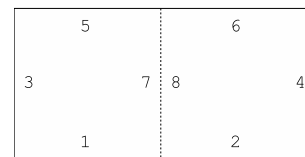


FIG. 3: The states in the bond basis of a brickwork plaquette. It is convenient to use the bond basis introduced in Ref. 7, that is  $|\pm\rangle = \frac{1}{\sqrt{2}}(|\alpha\rangle \pm \zeta|\beta\rangle)$  where  $|\alpha\rangle$  and  $|\beta\rangle$  are shown in Fig. 4 of Ref. 19 and  $\zeta$  represents the sign of the bond.

We set the bimodal problem for the brickwork lattice by placing negative bonds at random. To reduce the complexity, we perform gauge transformations as in Ref. 19 so that the negative (defect) bonds are vertical only. We classify plaquettes into four types as shown in Fig. 4.

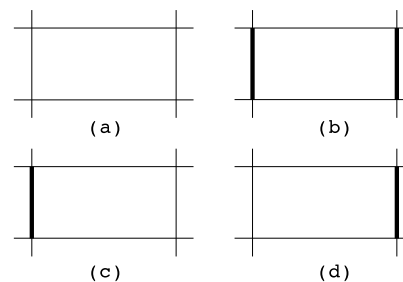


FIG. 4: Heavy lines denote negative (defect) bonds. There are four types of possible plaquettes after gauge transformation to vertical defect bonds. (a) and (b) are unfrustrated plaquettes while (c) and (d) are frustrated plaquettes.

To determine ground state properties, degenerate state perturbation theory is applied at arbitrarily small finite temperatures. We write exactly  $D = D_0 + \delta D_1$  where  $\delta = 1 - t$ , with  $t = \tanh(J/kT)$ , is used as a parameter for a perturbation expansion. The matrix  $D_0$  is singular and has defect eigenvectors  $|d\rangle$  corresponding to defect (zero) eigenvalue, that is  $D_0 |d\rangle = 0$ , localized on each frustrated plaquette, similar to those found for the square lattice<sup>19</sup>.

At first order the matrix  $D_1$ , which is  $2 \times 2$  block diagonal across bonds, is diagonalized in the basis of the defect eigenvectors. We also require the continuum Green's function  $G_c = (1 - P)g_c(1 - P)$  where  $P = \sum_d |d\rangle\langle d|$  and  $g_c = g_0 + g_0 U g_0$  with  $U$  defined similarly to Ref. 19. We can write  $g_c = g_{c1} + g_{c2}$  where  $g_{c1}$  has matrix elements connecting the basis states within a brickwork plaquette while  $g_{c2}$  connects only basis states across a single bond, that is  $g_{c2}(+, -) = -g_{c2}(-, +) = \frac{1}{2}$  and is only relevant for excited states. Although  $g_0$  can take us to the fermions associated with diluted bonds (labeled 7 – 8 in Fig. 3), it can be proven that these matrix elements do not effect the calculation of the partition function since  $D_1$  across that bond is equal to zero (there is no energy); we can disregard them. An alternative Pfaffian based on three nodes per site has been given in Ref. 17 but it cannot be adapted to our defect problem.

The matrix  $g_{c1}$  can be considered in the subspace with only six fermions (labeled 1 – 6 in Fig. 3) without any change of the gauge-invariant ground or excited state properties. We can also arrange to have  $g_{c1}$  orthogonal to defect states, that is  $g_{c1} |d\rangle = 0$ , by understanding that we can add any matrix  $A$  to  $g_{c1}$  as long as  $(1 - P)A(1 - P) = 0$ . This reduces the number of arithmetic operations for the calculation of excitations. The matrix  $g_{c1}$  can be presented for an unfrustrated plaquette as

$$g_{c1} = \frac{1}{2} \begin{bmatrix} 0 & -1 & 1 & -1 & s & s \\ 1 & 0 & 1 & -1 & s & s \\ -1 & -1 & 0 & -1 & s & s \\ 1 & 1 & 1 & 0 & s & s \\ -s & -s & -s & -s & 0 & 1 \\ -s & -s & -s & -s & -1 & 0 \end{bmatrix} \quad (4)$$

where  $s = 1$  for an unfrustrated plaquette with no negative bond (Fig. 4(a)) and  $s = -1$  for an unfrustrated plaquette with two negative bonds (Fig. 4(b)). The matrix  $U$  only occurs for plaquettes with two defect bonds. In detail,  $U_{34} = -U_{43} = -2$ . The matrix  $g_{c1}$  for a frustrated plaquette is given by

$$g_{c1} = \frac{1}{6} \begin{bmatrix} 0 & -2 & 2 & -1 & -s & 0 \\ 2 & 0 & 1 & -2 & 0 & s \\ -2 & -1 & 0 & 0 & -2s & -s \\ 1 & 2 & 0 & 0 & s & 2s \\ s & 0 & 2s & -s & 0 & 2 \\ 0 & -s & s & -2s & -2 & 0 \end{bmatrix} \quad (5)$$

where  $s = 1$  for a frustrated plaquette with a left negative bond (Fig. 4(c)) and  $s = -1$  otherwise (Fig. 4(d)). The

corresponding defect states are

$$|d\rangle = \frac{1}{\sqrt{6}} (|1\rangle + |2\rangle + |3\rangle + |4\rangle - s(|5\rangle + |6\rangle)) \quad (6)$$

The prefactor in Eq. (1) is essentially determined by the normalization of this vector.

At second order, we diagonalize  $D_2 = D_1 g_{c1} D_1$ . To continue for higher orders, we require the Green's functions  $G_r$ , as given in Ref. 7, obtained from previous orders; that is for states whose degeneracy has already been lifted. The general rule for  $D_r$  (at  $r$ th order) can be expressed as  $D_r = D_{r-1}(1 + G_{r-2} D_{r-2}) \dots (1 + G_1 D_1) g_{c1} D_1$ .

The calculation of the internal energy and the specific heat for the brickwork lattice is similar to the square lattice as described in Ref. 7. The internal energy is given by

$$U = \sum_{m=0}^{\infty} e^{-2Jm/kT} U_m. \quad (7)$$

where  $U_0$  is the ground state energy and  $U_m = -2^m J \text{Tr} R^m$ , for  $m > 0$ , and

$$R = D_1 g_{c1} (1 + D_1 G_1) (1 + D_2 G_2) \dots (1 + D_{r_{max}} G_{r_{max}}). \quad (8)$$

$r_{max}$  is the highest order of perturbation theory required.

However, there is one essential distinction between the square and brickwork lattices. Since we need three colors to color the brickwork lattice, this means that the color rules described in Ref. 7 are invalid and it follows that  $U_m \neq 0$  for all  $m$ . The specific heat per spin can be expressed in terms of the internal energy as

$$c_v = \frac{1}{N} \frac{dU}{dT} = \frac{1}{N} \left( \frac{2J}{kT^2} \right) \sum_{m=1}^{\infty} m e^{-2Jm/kT} U_m. \quad (9)$$

The degeneracy of the  $i$ th excited state is given as  $M_i$ . Expanding  $\ln Z$ , we get, for example,  $U_1 = 2J(\frac{M_1}{M_0})$  and  $U_2 = 4J(\frac{M_2}{M_0} - \frac{1}{2}(\frac{M_1}{M_0})^2)$ .

### III. RESULTS

Fig. 5 shows the distributions of  $\frac{M_1}{M_0}$  for the spin glass with  $(L+1) \times L$  spins. It is clear that the most likely value scales as the number of spins. We also consider a different shape of the patch boundary by changing the lattice size to  $(2L+1) \times L$  so that the equivalent hexagonal lattice has a more balanced shape. The distribution of  $\frac{M_1}{M_0}$  with  $(2L+1) \times L$  spins also shows again a most likely value that scales as the number of spins as shown in Fig. 6. Also, the value is roughly the same. In both cases, it is clear that the leading term of the specific heat grows like  $c_v \sim T^{-2} \exp(-2J/kT)$  indicating a  $2J$  excitation gap. Moreover, the distributions of  $\frac{M_1}{M_0}$  are extreme, do not self-average and are neither normal or lognormal. This is consistent with the square lattice as in Ref. 7.

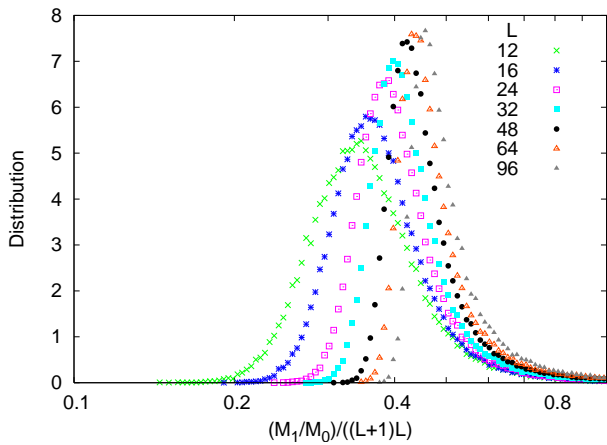


FIG. 5: (Color online) Distributions for  $\frac{M_1}{M_0} \frac{1}{(L+1) \times L}$  with various values of lattice size  $L$  with  $(L+1) \times L$  spins. Each distribution includes  $10^5$  disorder realizations, except for  $L = 96$  which has 30,000.

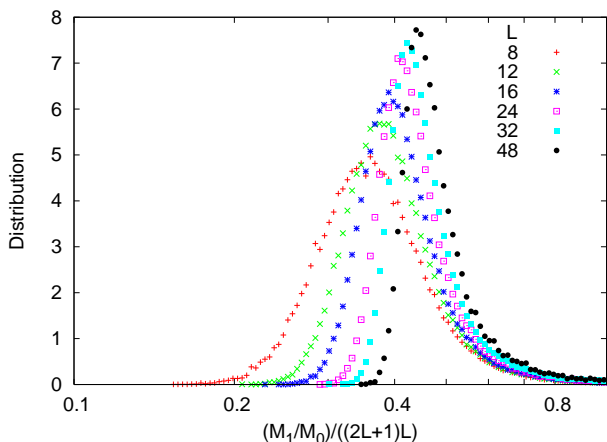


FIG. 6: (Color online) Distributions for  $\frac{M_1}{M_0} \frac{1}{(2L+1) \times L}$  with various values of lattice size  $L$  with  $(2L+1) \times L$  spins. Each distribution includes  $10^5$  disorder realizations.

The distributions of  $\frac{M_1}{M_0}$  clearly show extreme-value distributed properties with a fat tail. It is thus reasonable to analyze the distributions according to the Fréchet distribution with the probability density function:

$$f_{\xi, \mu, \beta}(x) = \frac{1}{\beta} \left( 1 + \xi \frac{x - \mu}{\beta} \right)^{-\frac{1}{\xi} - 1} \exp \left( - \left( 1 + \xi \frac{x - \mu}{\beta} \right)^{-\frac{1}{\xi}} \right) \quad (10)$$

where the parameters  $\mu$ ,  $\beta$  and  $\xi$  indicate location, shape and scale of the distribution respectively. The mode can be calculated by  $\bar{x} = \mu + \beta \frac{(1+\xi)^{-\xi} - 1}{\xi}$ . We estimate the parameters by a maximum likelihood estimator<sup>21</sup> to fit actual disorder realizations. It is found that the Fréchet distribution cannot fit exactly the peak of our actual distribution; the quality of the fit is quite poor and also deteriorates with respect to increasing  $L$ . An example for  $L = 48$  with  $(2L+1) \times L$  spins is shown in Fig. 7(a).

We have also tried to polish the fit using the Levenberg-Marquardt method<sup>22</sup> to fit the bin data, setting initial values of parameters equal to the values obtained from the algorithm of Hosking<sup>21</sup>. This provides alternative parameters and the curve is shown in Fig. 7(b). Although the quality of the fit looks a little better and the position of the mode somewhat improves, we are not convinced that Eq. (10) should necessarily describe the distribution exactly. For comparison, at different values of  $L$ ,

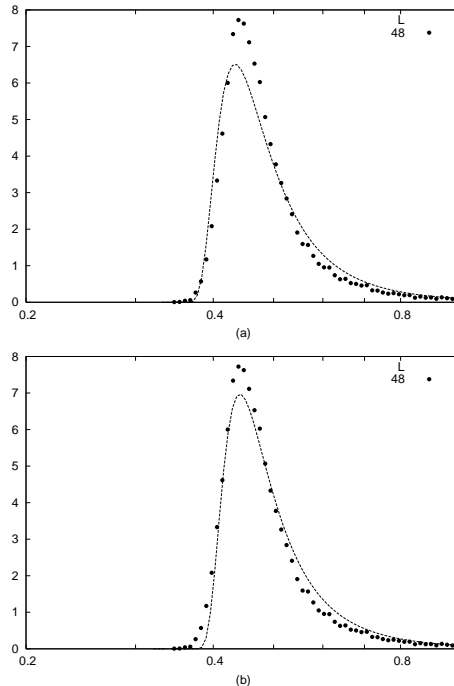


FIG. 7: Distributions for  $\frac{M_1}{M_0} \frac{1}{(2L+1) \times L}$  with  $L = 48$  and  $(2L+1) \times L$  spins. (a) The line uses the parameters obtained from the algorithm of Hosking<sup>21</sup> fitted to actual disorder realizations. (b) The line uses the parameters obtained from the algorithm of Levenberg-Marquardt<sup>22</sup> fitted to bin data using the Hosking parameters as initial values.

the fitted distributions divided by  $f(\bar{x})$  are shown in Fig. 8. It is also useful to present the mode of the fitted distributions as a function of  $L$  in Fig. 9. We trust that the mode converges; there is no reason to believe otherwise.

We have also found distributions for the second contribution to the internal energy,  $\frac{M_2}{M_0} - \frac{1}{2} \left( \frac{M_1}{M_0} \right)^2$ . These are shown in Figs. 10 and 11. The most likely value is very close to zero. The skewness also suggests the dominance of the first excitations. We thus believe that higher excitations are unlikely to change our conclusion that the energy gap is  $2J$ . The mode of  $\frac{M_2}{M_0}$  alone scales as  $((L+1)L)^2$  and  $((2L+1)L)^2$  as shown in Figs. 12 and 13, respectively.

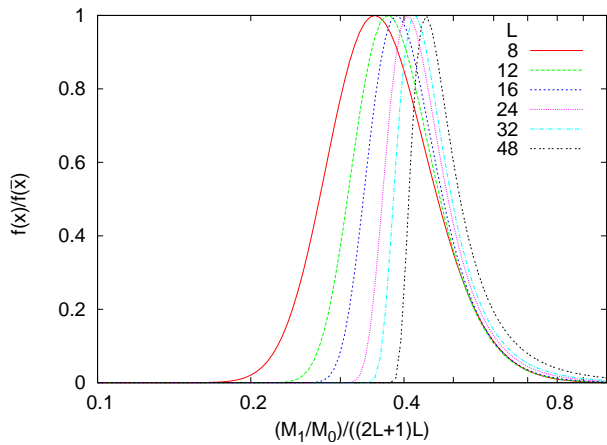


FIG. 8: (Color online) Fréchet distributions from fitting the bin data in Fig. 6 by the algorithm of Levenberg-Marquardt using the Hosking parameters as initial values.

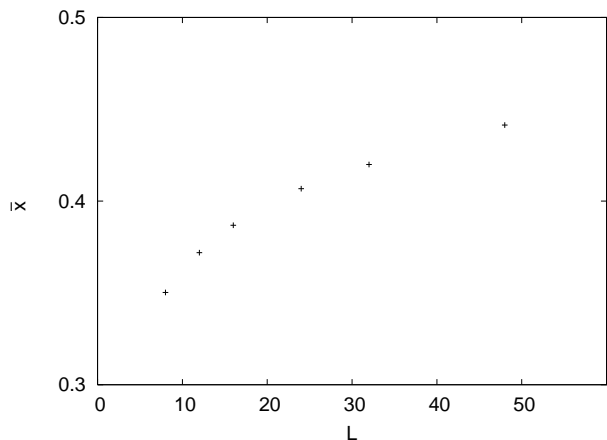


FIG. 9: The mode of the fitted distributions with various values of lattice size  $L$  with  $(2L + 1) \times L$  spins.

#### IV. CONCLUSIONS

In conclusion, we have reported exact results for the excitations of the bimodal Ising spin glass on the brickwork lattice by expanding in arbitrary temperature from the ground state. This is complimentary to the more usual extrapolation from finite temperature.

We find that the energy gap is  $2J$  for both finite and infinite lattices. The thermodynamic limit is trivial in contrast to the difficulties associated with the square lattice. Our result may suggest that a  $2J$  energy gap is universal for planar bimodal Ising spin glasses in the thermodynamic limit. For instance, the triangular lattice could very well be expected to behave similarly to the square lattice since its plaquettes can be colored using just two colors; the brickwork lattice requires three colors.

As a final note, we expect a correlation length  $\xi \sim \exp(2J/kT)$  in probable agreement<sup>2,7,8,23,24</sup> with the square lattice. Our reasoning is based on the construction

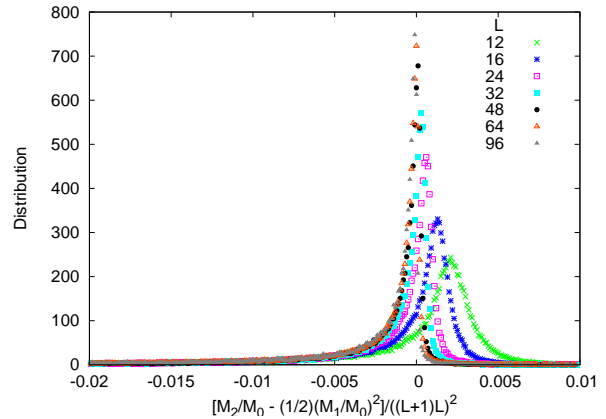


FIG. 10: (Color online) Distributions for the second term in the specific heat with various values of lattice size  $L$  with  $(L + 1) \times L$  spins. Each includes  $10^5$  disorder realizations, except for  $L = 96$  which has 30,000.

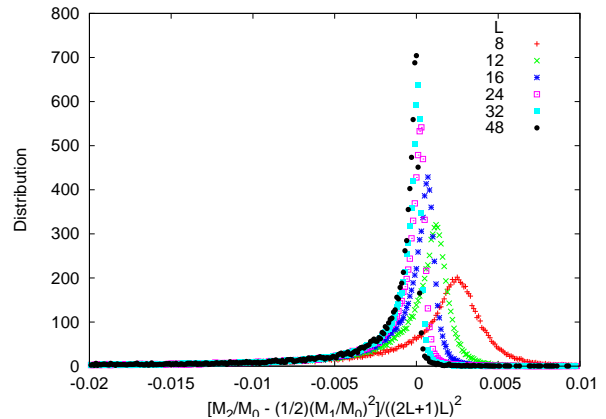


FIG. 11: (Color online) Distributions for the second term in the specific heat with various values of lattice size  $L$  with  $(2L + 1) \times L$  spins. Each includes  $10^5$  disorder realizations.

of correlation functions using reciprocal defects<sup>17,18,20</sup> and closed polygons. The essential point is that, for a finite lattice, the correlation functions must be analytical functions of  $t$  and thus of  $\delta \sim \exp(-2J/kT)$ . Comparison with the asymptotic expression  $\exp(-R/\xi)/R^\eta$  for correlation functions at large separation  $R$ , allows us to deduce that  $\xi^{-1}$  is also an analytical function of  $\delta$ . If the thermodynamic limit is trivial for the energy gap, then it is very likely to be so for the correlation length. It is also known that the fully frustrated brickwork lattice has a constant correlation length<sup>25</sup> and that the ground state is not critical, unlike the Villain model<sup>26</sup> that has a non-analytical free energy although  $\xi^{-1} \sim \delta$  nevertheless<sup>27</sup>.

#### ACKNOWLEDGEMENTS

W. A. thanks the Commission on Higher Education Staff Development Project, Thailand for a scholarship.

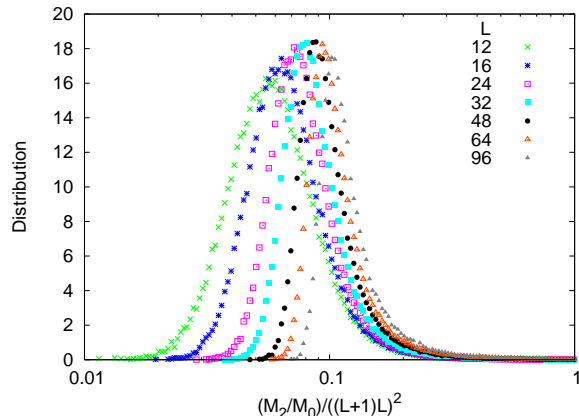


FIG. 12: (Color online) Distributions for  $\frac{M_2}{M_0} \left( \frac{1}{(L+1)L} \right)^2$  with various values of lattice size  $L$  with  $(L+1) \times L$  spins. Each distribution includes  $10^5$  disorder realizations, except for  $L = 96$  which has 30,000.

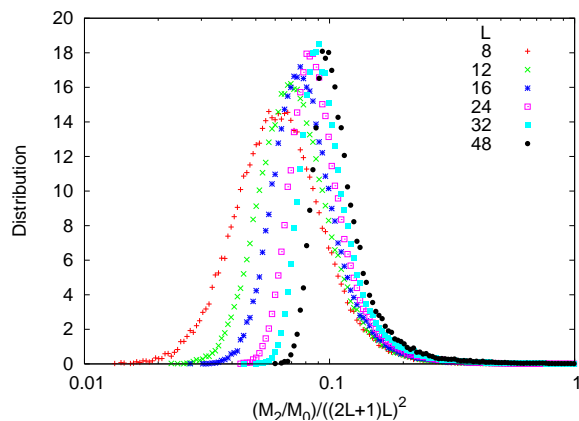


FIG. 13: (Color online) Distributions for  $\frac{M_2}{M_0} \left( \frac{1}{(2L+1)L} \right)^2$  with various values of lattice size  $L$  with  $(2L+1) \times L$  spins. Each distribution includes  $10^5$  disorder realizations.

Some of the computations were performed on the Tera Cluster at the Thai National Grid Center.

- 
- <sup>1</sup> A. K. Hartmann and A. P. Young, Phys. Rev. B **64**, 180404(R) (2001).  
<sup>2</sup> J. Houdayer, Eur. Phys. J. B **22**, 479 (2001).  
<sup>3</sup> J.-S. Wang and R. H. Swendsen, Phys. Rev. B **38**, 4840 (1988).  
<sup>4</sup> J. Lukic, A. Galluccio, E. Marinari, O. C. Martin, and G. Rinaldi, Phys. Rev. Lett. **92**, 117202 (2004).  
<sup>5</sup> J.-S. Wang, Phys. Rev. E **72**, 036706 (2005).  
<sup>6</sup> H. G. Katzgraber, L. W. Lee, and I. A. Campbell, cond-mat/0510668 (2005).  
<sup>7</sup> W. Atisattapong and J. Poulter, New J. Phys. **10**, 093012 (2008).  
<sup>8</sup> L. Saul and M. Kardar, Phys. Rev. E **48**, R3221 (1993); Nucl. Phys. B **432**, 641 (1994).  
<sup>9</sup> T. Jörg, J. Lukic, E. Marinari, and O. C. Martin, Phys. Rev. Lett. **96**, 237205 (2006).  
<sup>10</sup> H. G. Katzgraber, L. W. Lee, and I. A. Campbell, Phys. Rev. B **75**, 014412 (2007).  
<sup>11</sup> E. E. Vogel and W. Lebrecht, Z. Phys. B **102**, 145 (1997).  
<sup>12</sup> A. Aromsawa, Ph.D. Thesis, Mahidol University (2007).  
<sup>13</sup> J. Bendisch, Physica A **359**, 399 (2006).  
<sup>14</sup> S. L. A. de Queiroz, Phys. Rev. B **73**, 064410 (2006).  
<sup>15</sup> H. Nishimori and M. Ohzeki, J. Phys. Soc. Jpn. **75**, 034004 (2006).  
<sup>16</sup> M. Ohzeki, arXiv:0811.0464v1 (2008).  
<sup>17</sup> H. S. Green and C. A. Hurst, *Order-Disorder Phenomena* (Interscience, London, 1964).  
<sup>18</sup> J. A. Blackman, Phys. Rev. B **26**, 4987 (1982).  
<sup>19</sup> J. A. Blackman and J. Poulter, Phys. Rev. B **44**, 4374 (1991).  
<sup>20</sup> J. Poulter and J. A. Blackman, Phys. Rev. B **72**, 104422 (2005).  
<sup>21</sup> J. R. M. Hosking, Appl. Stat. **34**, 301 (1985).  
<sup>22</sup> W. H. Press, S. A. Teukolsky, W. T. Vetterling, and B. P. Flannery, *Numerical Recipes in Fortran* (Cambridge University Press, Cambridge, 1992).

- <sup>23</sup> H. G. Katzgraber and L. W. Lee, Phys. Rev. B **71**, 134404 (2005).
- <sup>24</sup> R. Sungthong and J. Poulter, J. Phys. A **36**, 6347 (2003).
- <sup>25</sup> W. F. Wolff and J. Zittartz, Z. Phys. B **49**, 139 (1982).
- <sup>26</sup> J. Villain, J. Phys. C **10**, 1717 (1977).
- <sup>27</sup> J. Lukic, E. Marinari, and O. C. Martin, Europhys. Lett. **73**, 779 (2006).